

Silicon Nanowires Obtained by Low Temperature Plasma-Based Chemical Vapor Deposition.

R. A. Puglisi*, G. Mannino, S. Scalse, A. La Magna
Consiglio Nazionale delle Ricerche, Istituto per la Microelettronica e Microsistemi, Strada
Ottava 5 Zona Industriale, 95121, Catania, Italy

V. Privitera
MATIS-IMM-CNR, Via Santa Sofia 64, Catania, Italy

*Corresponding author: Email: rosaria.puglisi@imm.cnr.it, Tel.: +39 0955968237, Fax: + 39
0955968312

ABSTRACT

Silicon Nanowires (Si-NWs) are obtained by vapor-liquid-solid growth using an inductively coupled chemical vapor deposition system which works at temperatures lower than 400 °C. Gold nanodots are used as metal catalyst. The selective growth of Si-NWs on the gold nanodots is obtained by controlling the contribution coming from the uncatalyzed growth on the bare Si substrate. In this way the final NW length can be controlled, and it is not influenced by the thickness of the uncatalyzed layer. The important parameter ruling the NW growth is found to be the plasma power which governs the dissociation of the Si precursor gas. Final NW lengths of 1 μm are obtained at temperatures of 380 °C with a thickness of uncatalyzed layer equal to zero. Also the NW density is addressed in this work and it is optimised by increasing the gold equivalent thickness. The NW density is increased from 2.9×10^8 to $1.3 \times 10^{10} \text{ cm}^{-2}$, when the gold equivalent thickness passes from 1.8 nm to 2.2 nm.

INTRODUCTION

Standard planar junctions of Si based solar cells suffer from low efficiency/cost ratio for many reasons mainly related to the capture and conversion of the solar energy and to the high manufacturing and production costs. The intrinsic nature of the planar junction is indicated as one of the possible reasons for the low conversion efficiency because in this architecture the charge carriers are collected along the same direction as light is absorbed [1]. Radial junctions formed in quasi one-dimensional (1D) structures can overcome this limitation because thanks to their innovative architecture they orthogonalise the light absorption from the carrier collection paths, enabling at the same time to increase the first parameter and reduce the second one. In this way the requirements about the electronic quality of the material used can be lowered and the costs decreased. Si-NWs are currently considered good potential candidates for the formation of radial junctions. Besides the light/current decoupling, they offer additional advantages like reduced light reflection, improved light trapping and the possibility to tune the band-gap [2-5]. For this application however the main Si-NWs morphological characteristics such as length, diameter and density have to be controlled and optimised. One of the most popular methods to form NWs is the vapor-liquid-solid growth on metallic catalysts [6-11]. In this method the Si precursors are deposited on the substrate where they can interact with i) the catalyst, and give rise to the formation of the NW, or ii) with the bare Si substrate, where they can diffuse or form a stable two-dimensional (2D) Si layer. For the first point to be effective, the catalyst surface has to be free of any oxide. To obtain this, many methods have been proposed in literature, like in-

situ cleaning at temperatures higher than 800°C to desorb the oxide layer, or the usage of hydrogen with plasma before and during the NWs deposition [12, 13]. If the Si precursor interacts with the catalyst clean surface the eutectic formation is promoted and the VLS can take place. For the second point, the formation of the Si NWs is the result of a compromise between the uncatalyzed growth of the 2D Si layer and the catalyzed growth of the 1D Si NWs. For this aspect the final effective length of the NWs can be reduced by the thickness of the 2D layer. We note that in order to maximise the visible light absorption, the photons must cross a Si thickness (i.e. the NWs length) of the order of microns. The other important aspect to be addressed for the application of radial junctions is related to the density of the NWs. It governs the effective photoactive area, i.e. the quantity of absorbed light, and then the amount of generated current. With NW diameter of about 20 nm and a separation between the NW walls of at least twice the diameter to allow proper conformal metal contact, the optimal NW density should be $\sim 1 - 2 \times 10^{10} \text{ cm}^{-2}$. Regarding the diameter of the NWs, the uncatalyzed deposition of Si on the NW side-wall can affect this parameter, by inducing tapering or creating an heterointerface between the crystalline Si core of the NW and the amorphous Si shell [14]. We demonstrate the formation of Si NWs at temperatures lower than 400 °C through a process where the uncatalyzed growth is controlled. The NWs are cylindrical, crystalline and present lengths up to about 1 μm while the thickness of uncatalyzed layer is equal to zero. The control on the formation of the continuous Si film deposition is pursued by properly tuning the plasma power, which at high levels promotes the decomposition of the Si precursor and then the efficiency of uncatalyzed deposition, while at low levels may affect the NWs growth rate. The NWs density is also optimised, by modifying the metal catalyst initial coverage. Final NWs densities higher than $1 \times 10^{10} \text{ cm}^{-2}$ are obtained by using equivalent metal thickness of 2.2 nm.

EXPERIMENTAL

The substrates used for the Si-NW deposition were p type 6" Si wafers. After a brief HF dip, Au nanodots of $1.8 \div 2.2 \text{ nm}$ of equivalent thickness were deposited by sputtering. The samples were then annealed for 30 min at 800°C in Ar and after a second HF dip they were loaded in the CVD chamber. The last HF dip was performed because samples analysed by TEM, after the sputtering step, presented a thin shell of oxide. This is attributed to an intermixing between the Au atoms and the Si atoms that creates a thin layer of Si on the surface of the gold dots. This layer reoxidizes in air and prevents the catalytic activity of Au. Before the deposition the Au dots density and average radius were respectively $1.5 \times 10^{11} \text{ cm}^{-2}$ and 6 nm. The deposition system used was the Inductively Coupled CVD Oxford Plasmalab 100. The substrates were heated at 380 °C for 1 h before the depositions, which were performed by using a mixture of SiH_4 and Ar, by fixing the deposition time to 900 s, and with power ranging between 20 and 1000 W. The samples were analyzed by using a ZEISS SUPRA35 Scanning Electron Microscopy (SEM), equipped with a field emission electron gun, and by Transmission Electron Microscopy (TEM) equipped with a system for Energy Filtering (EFTEM).

RESULTS

Figure 1 (a) shows the SEM micrograph in plan view of a typical substrate covered by Au nanodots used for the deposition of the NWs. It corresponds to a deposited equivalent thickness of gold equal to $t_{eq} = 1.8 \text{ nm}$. The white spots represent the Au nanodots and the black regions represent the uncovered Si substrate. In Figure 1 (b) it is reported the dot size distribution as a function of the dot radius calculated by the SEM analysis relative to the same sample and

obtained by considering a statistics of more than 500 dots. The graph shows that the distribution is peaked at about 5 nm with a range size between 2 and 20 nm. The total dot density results equal to $1.5 \times 10^{11} \text{ cm}^{-2}$ and the Au coverage is 23%.

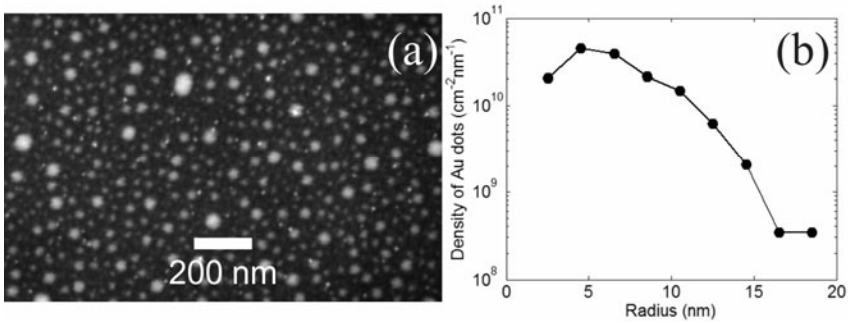


Figure 1. (a) SEM in plan view of the typical substrate used for the deposition of the Si-NWs. The black parts represent the uncovered Si substrate while the white regions represent the Au nanodots. In this case the gold deposited equivalent thickness corresponds to 1.8 nm. (b) Dot size distribution as a function of the dot radius relative to the sample in (a).

Figure 2 shows the SEM in cross section of two samples deposited at 1000 W (a) and 20 W (b). In the first case the density of Au nanodots was the same as in Figure 1, in the second case the dot density was very low, i.e. $9.4 \times 10^7 \text{ dot/cm}^2$. The very low density of catalyst seeds allows observing the regions of uncovered Si. In the first case, Figure 2 (a), a continuous rough Si layer is deposited on the substrate and no Si-NWs are present. The Au dots are buried under the 2D layer. The layer thickness is $135 \pm 10 \text{ nm}$. In the second case, Figure 2 (b), Si-NWs are deposited and no continuous Si layer is observed on the substrate in the regions outside the NWs. The result can be explained with the following argumentation: the low power plasma decreases the efficiency of SiH_4 decomposition giving raise to smaller contribution from the decomposition products SiH_x with $x < 3$, which present very high sticking coefficients (~ 1) and have the main role for the uncatalyzed deposition. The decomposition products with $x \geq 3$, which present lower sticking coefficients, decompose selectively on the Au dots and strongly enhance the formation of the NWs [15]. The rough isolated Si regions at the base of the NWs were observed by TEM analysis in cross view and were a mixture of crystalline Au and Si grains. They should be the result of the cooling process of the Au-Si eutectic phase after the deposition, during which the two materials separate and go to the stable crystalline phase.

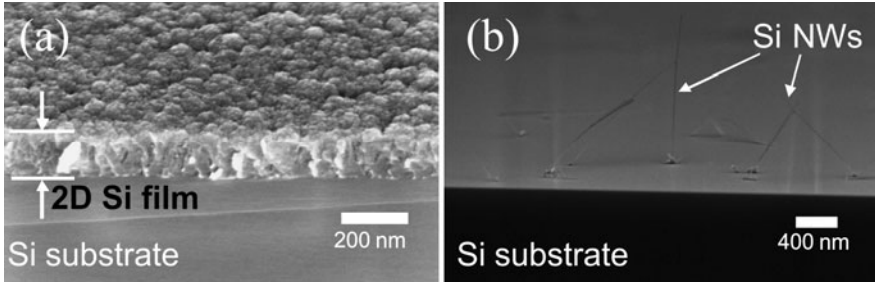


Figure 2. SEM micrographs in cross view on samples obtained at 1000 W (a) and 20 W (b) by fixing the other deposition parameters. In the first case it is visible a continuous rough Si layer deposited on the substrate, while in the second case it is possible to see the Si-NWs deposited on the Si substrate.

It should be noted that the responsible for the absence of 2D growth and the presence of Si-NWs in the result shown in Figure 2 (b) was the reduced plasma power and not the low density of Au dots. Indeed, Figure 3 (a) shows the sample deposited at 20 W on a Si substrate with dot density equal to that in Figure 2 (a), i.e. $1.5 \times 10^{11} \text{ cm}^{-2}$ and $t_{eq} = 1.8 \text{ nm}$. The NWs presented diameters ranging between 5 and 20 nm, and average lengths between $300 \div 400 \text{ nm}$. The density of the NWs measured in plan view is about $2.8 \times 10^8 \text{ cm}^{-2}$. Figure 3 (b) shows the sample deposited in the same conditions of Figure 2 (a), i.e. 20 W and $t_{eq} = 1.8 \text{ nm}$ of Au, but at a lower deposition temperature i.e. 250 °C, instead of 380°C. As it is possible to see NWs are present on the sample, but they are not straight and present a "worm-like" shape. Moreover the density of NWs is very low and many Au dots did not give rise to the growth of NWs. The presence of NWs at this deposition temperature is an unexpected result since it is known that, to form NWs through VLS mechanism by using gold as a catalyst, it is necessary to heat the sample at temperatures higher than the eutectic temperature of the Au-Si phase, which is 363 °C. The formation of NWs could be due to the lowering of the melting point of small gold dots which is estimated to be of about 140 °C less than the eutectic temperature for the bulk metal, for dots of about 10 nm in size [9].

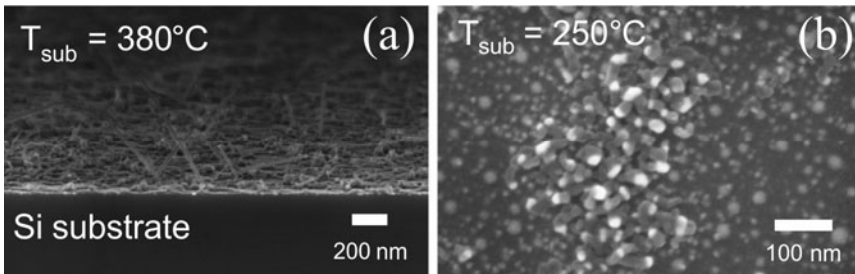


Figure 3. Si-NWs deposited at 380°C (a) and at 250 °C (b). It is possible to see that at 380 °C the NWs are straight, while at 250 °C they present a worm-like structure typical of very defective wires.

Figure 4 shows the high resolution TEM analysis on a Si-NW showing its crystalline structure and the metal tip at the top. The Si-NW diameter is equal to 3 nm.

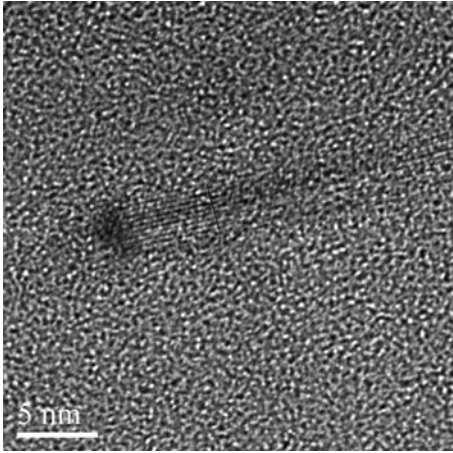


Figure 4. HRTEM on a Si-NW showing the crystalline structure of the NW and the metal tip at the top. The Si-NW diameter is equal to 3 nm.

Figures 5 (a) and (b) show the comparison between two samples deposited at 380 °C and 20 W on a substrate with $t_{eq} = 1.8$ nm and 2.2 nm respectively, observed in plan view by SEM. As it is possible to see the sample in Figure 5 (b) presents a much higher density of NWs with respect to the first case. The measured density in this case is $1.3 \times 10^{10} \text{ cm}^{-2}$. Figure 5 (c) presents a graph reporting the NW density as a function of Au equivalent thickness ranging between 1.8 and 2.2 nm, and it shows that the density increases with t_{eq} . It is worth noting that the control on the 2D growth has an impact also on the NW density, because it leaves visible to the precursor gas all of the catalyst seeds. Moreover, the NWs do not present any tapering or amorphous Si shells deposited on the side-walls, this again due to the suppression of uncatalyzed deposition of Si. Future work will focus on the process transfer on proper $\langle 111 \rangle$ substrates to obtain vertically aligned NWs and the optimization of the size distribution through the usage of low-cost lithographies such as that based on self-assembling of block copolymers [16].

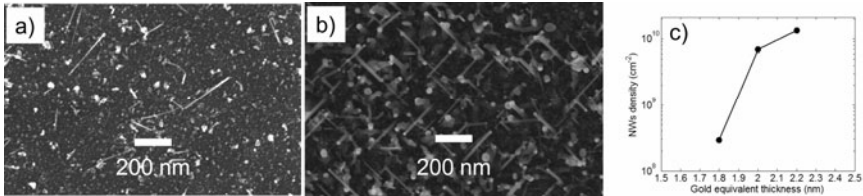


Figure 5. Si-NWs deposited on 1.8 nm (a) and 2.2 nm (b) of equivalent Au thickness,

observed in plan view by SEM. (c) Measured NWs density as a function of Au equivalent thickness present on the substrate before the deposition.

CONCLUSIONS

In conclusion a method to fabricate crystalline Si NWs with controlled length and density is reported. The growth is obtained by VLS on Au nanodots at 380 °C through plasma based CVD of SiH₄. The competition between the 2D and 1D growth is controlled by tuning the plasma power. In particular the 2D growth is suppressed by decreasing the plasma power to activate only the selective decomposition of the SiH₄ on the catalyst. The NW density is increased by properly increasing the initial Au equivalent thickness. Final NW densities of $1.3 \times 10^{10} \text{ cm}^{-2}$ are obtained by using 2.2 nm of equivalent thickness.

ACKNOWLEDGMENTS

The authors wish to thank Markus Italia, Salvatore Di Franco and Corrado Bongiorno (CNR-IMM) for valuable help and expert support in several stages of the samples preparation and analysis.

REFERENCES

- [1] N. S. Lewis, *Science* 315, 798 (2007).
- [2] E. C. Garnett, M. L. Brongersma, Y. Cui, M. D. McGehee, *Ann Rev. Mater. Res.* 41, 269 (2011).
- [3] A. Fontcuberta i Morral, J. Arbiol, J. D. Prades, A. Cirera, and J. R. Morante, *Adv. Mater.* 19, 1347 (2007).
- [4] B. M. Kayes, H. A. Atwater, N. S. Lewis, *J. Appl. Phys.* 97 (11) 114302 (2005).
- [5] S. Perraud, S. Poncet, S. Noël, M. Levis, P. Faucherand, E. Rouvière, P. Thony, C. Jaussaud, and R. Delsol, *Sol. Energy Mater. Sol. Cells* 93, 1568 (2009).
- [6] R. S. Wagner, W. C. Ellis, *Appl. Phys. Letters* 4, 89 (1964).
- [7] E.I. Givargizov, *J. Cryst. Growth* 31, 20 (1975).
- [8] B.Z. Tian, X. L. Zheng, T. J. Kempa, Y. Fang, N. F. Yu, G. H. Yu, J. L. Huang, C. M. Lieber, *Nature* 449 (7164) 885-U8 (2007).
- [9] H. Suzuki, H. Araki, M. Tosa, T. Noda, *Mat. Trans.* 48 (8) 2202 (2007).
- [10] A. Irrera, E. Pecora, and F. Priolo, *Nanotechnology* 20, 135601 (2009).
- [11] M. Monasterio, A. Rodriguez, T. Rodriguez, and C. Ballesteros, presented at 2011 MRS Fall Meeting, Boston, MA, 2011.
- [12] I. Zardo, L. Yu, S. Conesa-Boj, S. Estradè, P. J. Alet, J. Rossler, M. Frimmer, P. Roca i Cabarrocas, F. Peirò, J. Arbiol, J. R. Morante, and A Fontcuberta i Morral, *Nanotechnology* 20, 155602 (2009).
- [13] I. Zardo, S. Conesa-Boj, S. Estradè, L. Yu, F. Peiro, P. Roca i Cabarrocas, J.R. Morante, J. Arbiol, and A. Fontcuberta i Morral, *Appl. Phys. A* 100, 287 (2010).
- [14] Y. Qin, F. Li, D. Liu, H. Yan, J. Wang, and D. He, *Materials Letters* 65, 1117 (2011).
- [15] "Suppression of the 2D growth during the synthesis of Si nanowires by Inductively Coupled Chemical Vapor Deposition", R. A. Puglisi, G. Mannino, S. Scalese, A. La Magna, V. Privitera, submitted to APL.
- [16] C. Garozzo, R. A. Puglisi, C. Bongiorno, S. Scalese, E. Rimini, and S. Lombardo, *J. Mater. Res.* 26 (2), 240 (2011).